Geophysical Research Letters

RESEARCH LETTER
10.1029/2021GL094716

Key Points:

- Impact of assimilating Aeolus winds in the ECMWF system from May to September 2020 is coupled to the easterly QBO phase
- Aeolus assimilation modifies the representation of vertically propagating Kelvin waves in the tropical UTLS
- Forecast improvements in May 2020 could be associated with the alteration in the upward-propagating Kelvin waves

Supporting Information:

Supporting Information may be found in the online version of this article.

Correspondence to:

N. Žagar,
nedjeljka.zagar@uni-hamburg.de

Citation:

Žagar, N., Rennie, M., & Isaksen, L. (2021). Uncertainties in Kelvin waves in ECMWF analyses and forecasts: Insights from Aeolus observing system experiments. *Geophysical Research Letters*, *48*, e2021GL094716. https://doi.org/10.1029/2021GL094716

Received 17 JUN 2021
Accepted 2 NOV 2021

Author Contributions:

Conceptualization: N. Žagar
Methodology: N. Žagar, M. Rennie, L. Isaksen
Validation: N. Žagar, M. Rennie, L. Isaksen
Visualization: N. Žagar, M. Rennie, L. Isaksen
Writing – original draft: N. Žagar
Writing – review & editing: N. Žagar, M. Rennie, L. Isaksen

Uncertainties in Kelvin Waves in ECMWF Analyses and Forecasts: Insights From Aeolus Observing System Experiments

N. Žagar[1], M. Rennie[2], and L. Isaksen[2]

[1]Meteorological Institute, Center for Earth System Research and Sustainability, Universität Hamburg, Hamburg, Germany, [2]European Centre for Medium-Range Weather Forecasts, Reading, UK

Abstract The European Space Agency Earth Explorer mission Aeolus with the first spaceborne Doppler Wind Lidar onboard provides global coverage of wind profiles twice per day. This paper discusses the impact of assimilating Aeolus winds on the quality of tropical analyses and forecasts using the observing system experiments of the European Centre for Medium-Range Weather (ECMWF). Presented examples show that Aeolus wind profiles bring changes to the Kelvin wave structure in the layers with a significant vertical shear during the easterly phase of the quasi-biennial oscillation in the period May to September 2020. Comparing Kelvin waves in analyses and forecasts with and without Aeolus winds, it is argued that improved ECMWF forecasts in the tropical tropopause layer are due to vertically propagating Kelvin waves.

Plain Language Summary The tropics are the region with the largest uncertainties in the initial states for numerical weather prediction, called analyses. Analysis uncertainties are largest in the tropical upper troposphere and the lower stratosphere (UTLS). One of the reasons is a lack of wind profiles which are more useful than temperature profiles in the tropics. This classical effect was described by Smagorinsky as "Not all data are equal in their information-yielding capacity. Some are more equal than others." ESA's ongoing Aeolus mission provides the first global wind profile observations from space. Despite their small number and relatively large random error, Aeolus winds have a positive impact on the quality of global weather forecasts, especially in the UTLS. In this paper, we discuss the impact of the Aeolus winds in UTLS focusing on the vertically propagating Kelvin waves, which are a major contributor to tropical variability. Several case studies are presented using the ECMWF model and data assimilation with and without Aeolus winds. The studied period May to September 2020 was characterized by a weakening easterly phase of the quasi-biennial oscillation (QBO). Results suggest that a stronger impact of Aeolus winds in May than later in summer was associated with the QBO and the background flow.

1. Introduction

Even though progress in numerical weather prediction (NWP) in the past two decades has been tremendous (Bauer et al., 2015), including progress in the simulation of tropical variability (Vitart et al., 2014), the tropics remain a region with the largest analysis uncertainties. This is particularly true in the upper troposphere and lower stratosphere (UTLS), where tropical analysis and short-range forecast uncertainties far exceed uncertainties in the upper troposphere in midlatitudes (e.g., Baker et al., 2014; Park et al., 2004; Žagar, 2017). For example, an intercomparison of the six state-of-the-art NWP systems by Park et al. (2004) showed that the root-mean-square differences between the analyses over the tropics exceeded the climatological standard deviation of the tropical circulation. In contrast, the differences among the same analyses over the extratropics make around 10% of the corresponding climatological variability. It is therefore not surprising that the description of synoptic variability in the tropical tropopause layer (TTL) is not reliable. Since variability of the tropical lower stratosphere is largely maintained by vertically propagating equatorial waves, their accurate representation in analyses is vital also for climate model validation (e.g., Fujiwara et al., 2012).

Analysis uncertainties in the tropics are associated with a lack of observations, especially observations of wind profiles, as well as with model errors and shortcomings in data assimilation modeling (e.g., Baker et al., 2014; Žagar et al., 2016). In this paper, we discuss the impact of the assimilation of the first spaceborne

measurements of global wind profiles by the Doppler Wind Lidar ALADIN (ESA, 1999, 2008; Reitebuch, 2012), onboard the ESA Earth Explorer mission Aeolus, on the quality of tropical analyses and forecasts in the European Centre for Medium Range Weather Forecasts (ECMWF) system. The Aeolus mission (Stoffelen et al., 2005) has been under development since the late 1990s leading to the successful launch of the Aeolus satellite in August 2018. At ECMWF, Aeolus observations have been used in operations since January 09, 2020. Prior to its operational use, a major effort was invested to validate the new measurements and to understand the origin of biases. After applying corrections for the bias, the random error of Aeolus observations in clear air is still typically about twice that of radiosondes or aircraft wind measurements, because the effective Aeolus laser signal was a factor 2–3 lower than expected prelaunch. Nevertheless, evaluation of the Aeolus forecast impact in the ECMWF operational system and observing system experiments show Aeolus' positive impact on short-range forecasts in the tropical UTLS region, with improvements in lower-stratosphere temperature forecasts extending to the medium range (Rennie et al., 2021). This was only the case after the discovery of a strong link between onboard telescope temperatures and systematic wind speed errors and its correction (Rennie & Isaksen, 2020; Rennie et al., 2021). Aeolus not only led to forecast improvements at several global NWP centers, but was also shown capable of observing gravity waves (Banyard et al., 2021) and providing useful aerosol observations (Baars et al., 2021).

Here, we present the first evidence that reported improvements in the simulations of tropical circulation are associated with a representation of the large-scale equatorial waves in UTLS, in particular the Kelvin wave. First, we show that Aeolus wind profiles improve the fit of short-term tropical forecasts to observations for other observations types, in spite of their random errors on average being significantly greater than error estimates for short-term tropical forecasts using the ensembles. We focus on analysis improvements in vertically propagating equatorial waves in the UTLS region and specifically on the Kelvin wave. By filtering the Kelvin waves from the ECMWF analyses with and without Aeolus winds, we demonstrate that Aeolus brings changes to the vertical wave structure in the layers with the strongest wind shear that is observed by Aeolus.

The Kelvin wave (KW) is the slowest eastward-propagating wave solution of the linearized primitive equations and therefore the first-order ingredient of the circulation response to tropospheric heating perturbations (e.g., Salby & Garcia, 1987), and is easily detectable in different types of observations (e.g., Alexander & Ortland, 2010; Kim & Alexander, 2013; Wheeler & Kiladis, 1999). In the stratosphere, where the KW was first discovered as a 15-day wave (Wallace & Kousky, 1968), it affects zonal mean quasi-periodic flows such as the quasi-biennial oscillation (QBO) (Baldwin et al., 2001), and it is widely considered to play a role in the dynamics of the Madden-Julian Oscillation (MJO) (Zhang, 2005). Although the KW is predominantly a planetary-scale wave (zonal wavenumber 1), it makes a significant contribution to tropical analyses uncertainties and forecast errors. The role of KWs in tropical weather predictability has been addressed by several studies in the past (Žagar, Buizza, et al., 2015; Žagar et al., 2007, 2013). For example, Žagar et al. (2007) found that the ECMWF forecast errors within the 20°N–20°S belt project on KWs significantly more in the easterly QBO phase than in the westerly phase. Žagar et al. (2016) showed that although the upper-troposphere tropical forecast errors grow more rapidly in the equatorial Rossby (balanced) modes, the analysis increments at the same levels are larger in unbalanced (non-Rossby or inertia-gravity) modes, including the KWs, suggesting shortcomings in the analysis of unbalanced tropical circulation. Furthermore, Žagar, Buizza, et al. (2015) showed that missing variance associated with KWs explains a large part of underdispersiveness of the ECMWF ensemble prediction system in the medium range in the tropics. It is unclear how well KW dynamics is represented in global climate models, as they still poorly simulate the QBO and MJO, and their connections (e.g., Kim et al., 2020).

Here, we use the ECMWF observing system experiments (OSEs) to investigate the impact of assimilating Aeolus winds on the Kelvin waves in the UTLS. This is carried out by applying a wavenumber decomposition of OSEs analyses and forecasts using classical linear wave theory, as presented in Section 2. We show the evidence of a positive impact of Aeolus winds on the tropical forecasts, followed by presentation of changes in KW analyses due to the assimilation of Aeolus winds. Section 4 contains the discussion and outlook.

2. Methods and Data

2.1. Observing System Experiment With Aeolus Winds

The ALADIN instrument onboard Aeolus measures profiles of the horizontal line of sight (HLOS) winds from the backscattering of molecules (Rayleigh winds) and of aerosols (Mie winds). For each channel, the profile is classified as clear or cloudy depending on the presence of the cloud particulates (Tan et al., 2008). Only Rayleigh-clear and Mie-cloudy profiles are used here. Individual measurements with horizontal scale of about 3 km are accumulated to produce profiles representing up to 86-km scale for Rayleigh-clear, and about 12 km for Mie-cloudy profiles. In the vertical direction, the atmosphere is divided into 24 layers, so-called range-bins, that have thickness of 250–2,000 m, and the HLOS wind is assigned to the half-way up the range bin. The Rayleigh-clear winds with large estimated observation error are rejected based on the limit of 12 m/s (8.5 m/s) above (below) 200 hPa. After applying a bias correction, the random error of Aeolus observations in clear air is found to vary between 4 and 7 m/s for Rayleigh-clear winds and 2.8–3.6 m/s for Mie-cloudy winds (Rennie et al., 2021). In the presented OSEs, the Rayleigh-clear winds below 850 hPa were discarded.

The OSE was performed for the period from mid-April to September 2020 using the operational ECMWF system with 137 levels up to 1 Pa. The model version was CY47R1.1 with 12-hr continuous 4D-Var (Lean et al., 2021) and an outer loop with a resolution TcO399 which corresponds to about 30-km grid distance. The magnitude of the background errors at model levels in the UTLS, that is estimated from the spread of the ensemble of 4D-Var analyses, varies between 1 and 3 m/s (not shown). The experiment which included Aeolus winds on top of all other observations is denoted "Aeolus." The reference experiment with all observations except Aeolus will be referred to as "NoAeolus." The largest analysis increments in the tropical zonal wind occur in the layer 200-100 hPa. For example, in the analysis cycle in mid-May discussed in Section 3, the mean magnitude of zonal wind increments at Aeolus geolocations in the NoAeolus cycle is 1.28 m/s compared to 1.41 m/s in the case with Aeolus winds included in the assimilation (not shown). Rennie et al. (2021) presented the NWP impact assessment for the whole OSE period. Here, we look at the Kelvin wave analyses in relation to the background flow.

2.2. Kelvin Wave Filtering

The KW is filtered from Aeolus and NoAeolus analyses using the MODES software (Žagar, Kasahara, et al., 2015) which implements linear wave decomposition in the terrain-following σ coordinate system following Kasahara and Puri (1981). MODES performs a multivariate projection of the horizontal winds and pseudo-geopotential field, which is defined by temperature and surface pressure, on balanced and unbalanced eigensolutions of the linearized primitive equations. The framework is well suited for the KW which is a normal mode of the global atmosphere. For details of the linear wave theory and decomposition, the reader is referred to Andrews et al. (1987) and Kasahara (2020), and references therein. The equatorial wave filtering of operational ECMWF forecasts at https://modes.cen.uni-hamburg.de reveals the KW signals regularly propagating eastward and upward to the stratosphere, as illustrated in Supporting Information S1. The strongest tropospheric KW signal is found over the Indian ocean and western Pacific as reported in earlier studies of KWs in reanalysis data and operational ECMWF analyses (Blaauw & Žagar, 2018; Suzuki et al., 2010; Wheeler et al., 2000).

Figure 1 shows the differences between the KW zonal winds in Aeolus and NoAeolus analyses during the period May to September 2020. It shows that the differences are larger in the eastern than in the western hemisphere. The largest differences are up to ±4 m/s which is 2–3 times greater than the average magnitude of the zonal wind analysis increments in the UTLS. Similar to the KW dynamics (Blaauw & Žagar, 2018; Flannaghan & Fueglistaler, 2012; Suzuki et al., 2010), there are periods of 1–3 weeks duration when the Aeolus-NoAeolus differences in the TTL layer are pronounced (levels at 83 and 108 hPa). In particular, mid-May 2020 is characterized by the largest difference at 83 hPa and we look at this case in more details in the next section.

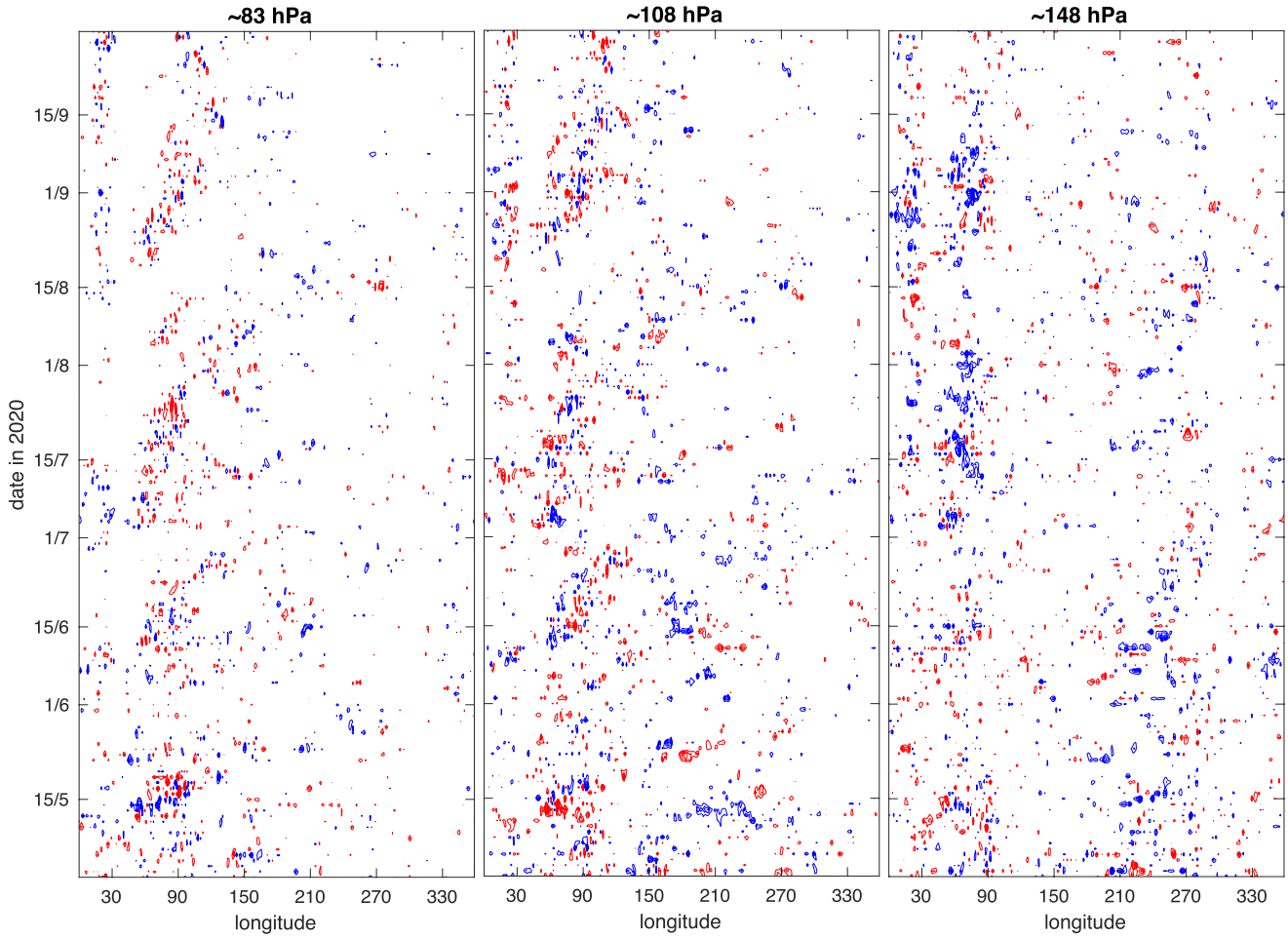

Figure 1. Kelvin wave zonal wind differences along the latitude 0.5°N between the 12 UTC analyses in Aeolus and NoAeolus experiments during the period May 01–September 30, 2020. Contouring is every 0.4 m/s, starting at ±0.8 m/s. Red contours for positive, and blue for negative differences.

2.3. Impact on Forecasts

Evidence of the impact of Aeolus winds on forecasts is presented in Figure 2 for the tropical belt 20°S–20°N at 100 hPa level. The difference in root-mean-square errors (rmse) in Aeolus and NoAeolus experiments compared to their respective analyses is normalized by the Aeolus experiment rmse for three months: May, June, and August 2020. A relative improvement in the Aeolus experiment compared to NoAeolus is shown

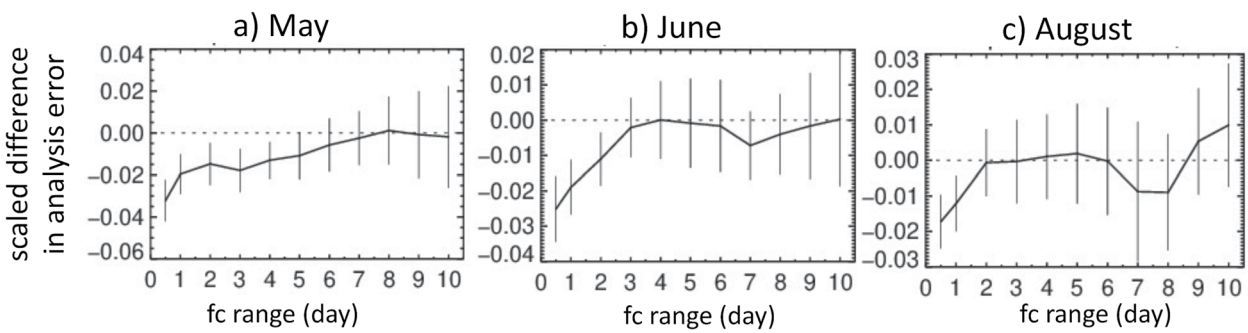

Figure 2. Normalized difference of the root-mean-square errors (rmse) of forecasts minus respective analyses for zonal winds in the tropics at 100 hPa. The difference is taken between the rmse of Aeolus and NoAeolus experiments and the normalization is by the rmse of the Aeolus experiment. The error bars for 95% confidence intervals are included.

as negative values of the normalized rmse. The period from May to August was characterized by weakening easterly shear lines in the lower stratosphere associated with the easterly phase of the QBO. Figure 2 shows that statistically significant forecast improvement by Aeolus winds diminished from 5–6 days in May to 3–4 days in June and 2–3 days in August. We speculate that this effect is associated with Aeolus' effects on vertically propagating equatorial waves during the easterly QBO phase and seasonal changes in the balanced upper tropospheric easterlies than can explain the longitudinal structure of the KW zonal wind (e.g., Baldwin & Gray, 2005; Suzuki et al., 2010).

In the troposphere, the balanced winds in May were westerly except over the Indian ocean, while easterlies dominated during July to September period throughout the tropics. The upper troposphere easterlies, which are on average found over the western Pacific, act as an escape window for KWs throughout the year and largely explains their longitudinal structure (Flannaghan & Fueglistaler, 2013). Links to the movies with the Kelvin waves and balanced winds in the operational ECMWF analyses in the upper troposphere and stratosphere are provided in Supporting Information S1 and can also be seen on the MODES webpage. In the next section, we use examples of KW profiles in May 2020 to discuss the importance of the QBO phase and the background winds for the analyses. The rmse of observation minus background for the period in May is provided in Supporting Information S1.

3. Aeolus Winds and the Equatorial Kelvin Wave

3.1. Kelvin Wave Winds Versus Balanced Winds Near the Equator

KW zonal winds superimposed on tropical balanced zonal winds in the Aeolus experiment in mid-May 2020 are displayed in Figure 3. The figure shows balanced westerlies in the upper tropical troposphere and within the TTL (approximately the layer 200-70 hPa), except between 60°E and 100°E. In this region, KW winds are about equal or stronger than the balanced wind, which are also easterlies. The predominant feature of Figure 3 is a strong shear of the balanced zonal wind, both vertical and longitudinal. The presence of a strong easterly wind shear layer between 100 and 80 hPa in May 2020 is associated with the easterly QBO phase which is known to provide favorable conditions for intense KW dynamics (Flannaghan & Fueglistaler, 2012; Suzuki et al., 2010).

An eastward-slanted, vertically propagating KW structure over the Indian ocean (60°–90°E) in Figure 3 in the vicinity of the strongest balanced easterlies is similar to the typical KW structure in observations and earlier ECMWF analyses (e.g., Alexander & Ortland, 2010; Blaauw & Žagar, 2018; Flannaghan & Fueglistaler, 2013; Suzuki & Shiotani, 2008). Similarly, a weaker KW signal below 100 hPa over the western Pacific is a known property of KWs in regions with westerly balanced flow. An equivalent of Figure 3 for the NoAeolus experiment is provided in Supporting Information S1. Other figures in Supporting Information S1 for the same three days show that KWs represent most of the unbalanced (or non-Rossby) signal. The total zonal flow appears far less smooth than the balanced winds because small-scale, divergent structures project on the inertia-gravity modes.

Figure 3 also shows that between May 13 and May 16, 2020, balanced easterlies over the Indian ocean strengthened, along with strengthening westerlies around the dateline. An even stronger enhancement of both horizontal and vertical shear can be seen in the total wind (Figure in Supporting Information S1) since the KW easterlies (westerlies) occur in the regions of balanced easterly (westerly) flow. Such strong wind shear is typical for midlatitude fronts and simulated Aeolus winds were demonstrated capable of improving frontal features (Šavli et al., 2018). On synoptic scales in midlatitudes, the thermal wind balance can be applied to derive the vertical wind shear from the horizontal temperature gradient, with the temperature field obtained from high-accuracy measurements of radiances. In the tropics, the weak-temperature gradient theory for the slow, large-scale motions relies on the smallness of the temperature gradient (Sobel et al., 2001), thereby excluding the KW. However, wherever the Kelvin and Rossby waves are present together near the equator, their zonal winds will sum up (or subtract) whereas their temperature perturbations will subtract (or sum up), since their mass-wind couplings have opposite signs. Using the horizontal structure of mass-field observations to derive the Kelvin and Rossby wave signals near the equator therefore requires quantification of their respective forecast-error variances. This is a challenging task for data assimilation,

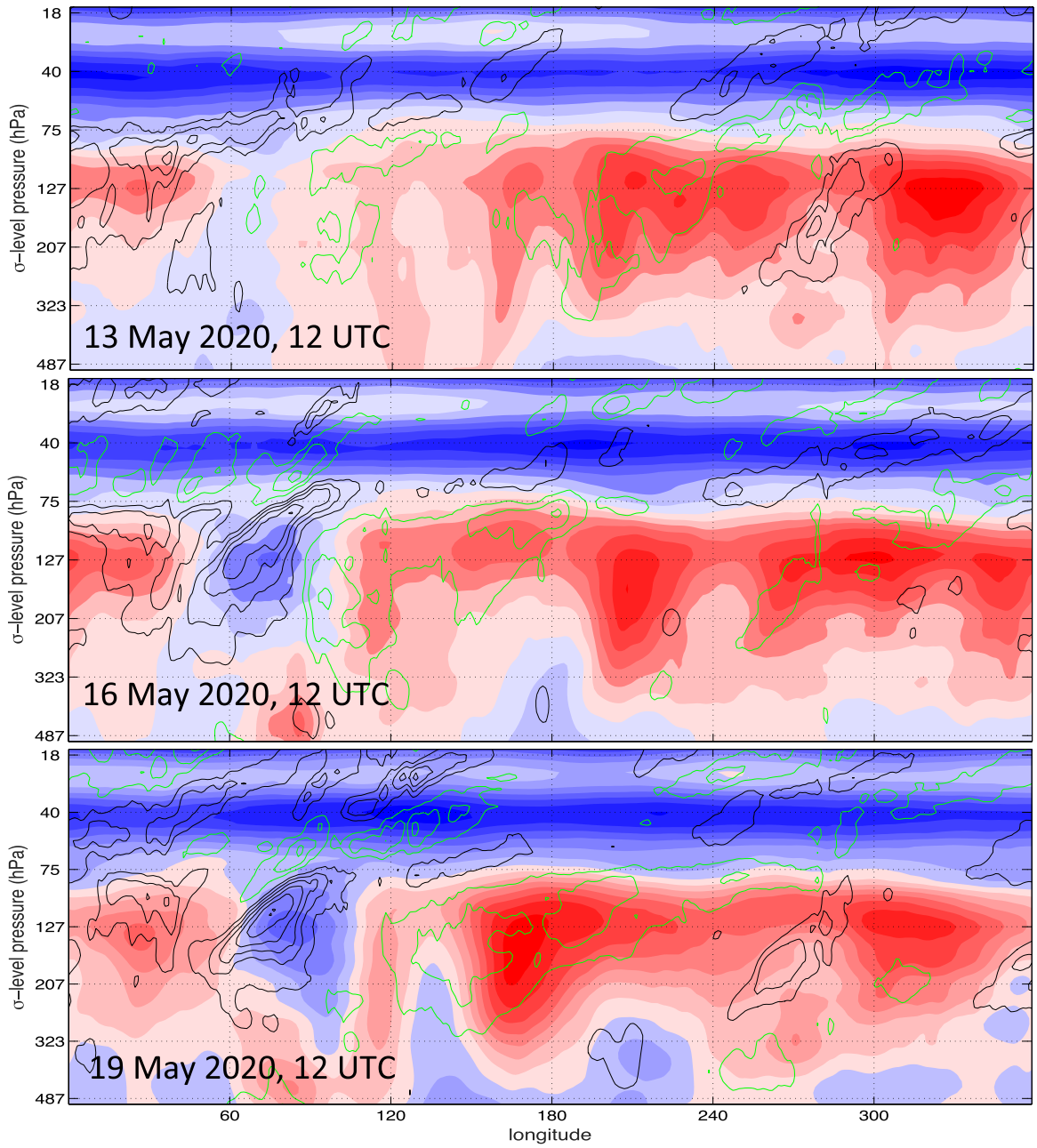

Figure 3. Kelvin wave zonal winds (contours) superposed on the balanced winds (shades) in Aeolus experiments on May 13, May 16, and May 19, 2020, 12 UTC. Winds are averaged over the belt 10°N–10°S. Contouring is every 3 m/s, starting at ±3 m/s, with green contours for westerly and black contours for easterly Kelvin wave zonal winds. Balanced zonal winds are shaded every 3 m/s, with red shades for westerlies and blue shades for easterlies. The pressure labels on the *y* axis are rounded values of σ multiplied by 1013.25 hPa.

even in the perfect-model 4D-Var (Žagar et al., 2008). Direct wind observations, as argued since early days of the Aeolus project, are crucial to improve accuracy of tropical analyses.

3.2. Effects of Aeolus Winds on Kelvin Waves

There is little difference between the outputs of Aeolus experiments in Figure 3 and an equivalent figure for NoAeolus experiment, which is shown in Supporting Information S1. Differences are up to the level used for contouring, 3 m/s, which is not a small value for an experiment in which the only difference is

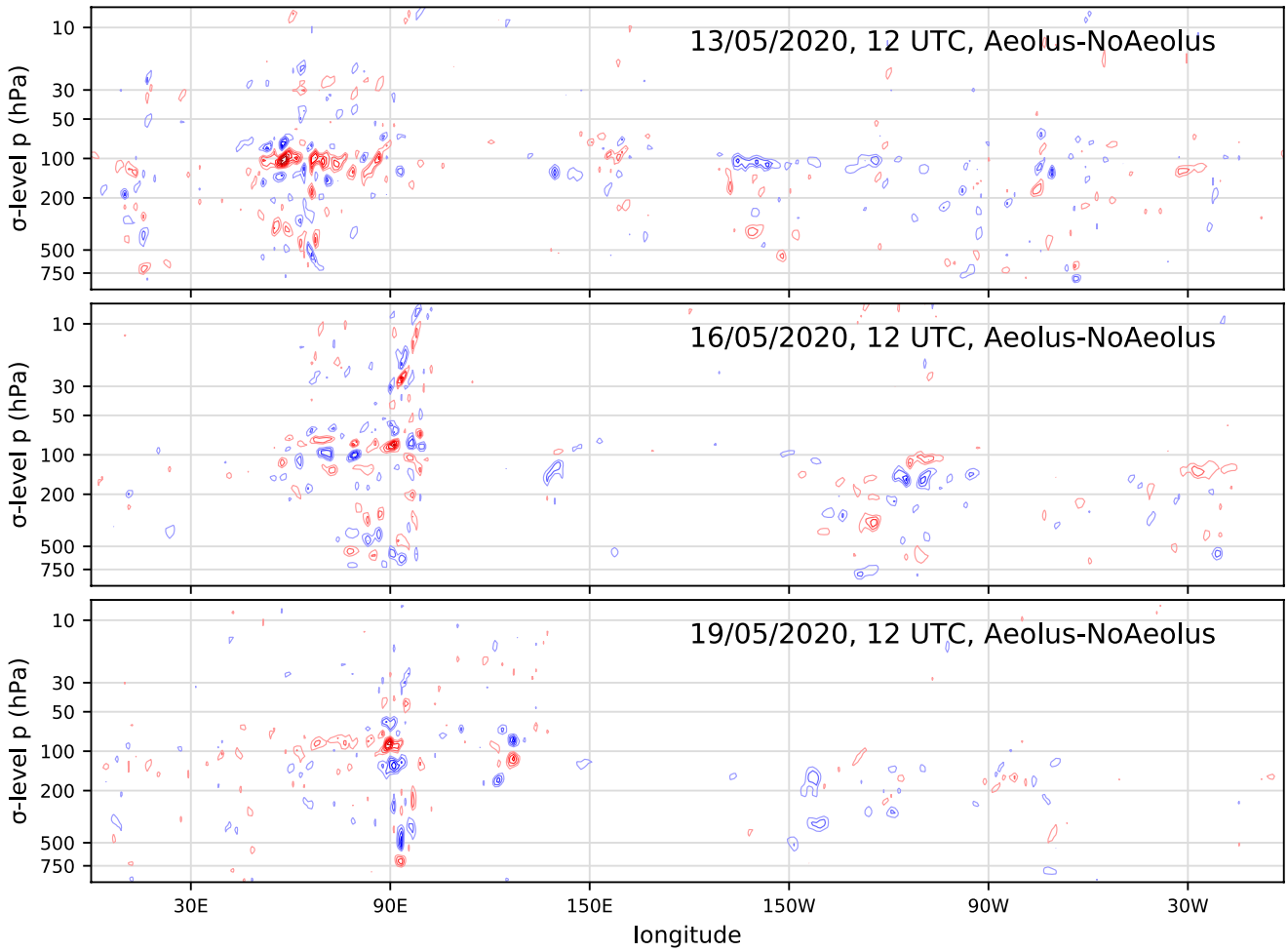

Figure 4. Kelvin wave zonal wind differences along the latitude 0.5°N between the Aeolus and NoAeolus experiments on May 13, May 16, and May 19, 2020, 12 UTC. Contouring is every 0.5 m/s, starting at ±1 m/s. Red contours for positive, and blue for negative differences.

the assimilation of Aeolus winds. Although Aeolus winds are characterized by a significant random error for the Rayleigh-clear profiles, the Mie-cloudy winds in tropical cirrus layer (top of convection) have errors 2–3 m/s, similar to that of radiosondes. To understand tropical dynamical processes affected by Aeolus assimilation, we need to look at differences between analyses or at analysis increments. The latter shows the effect of observations in a single assimilation cycle whereas the former includes the effect of observations assimilated also in the earlier cycles. The memory of observations in the tropics should be longer than in the extratropics (Fisher et al., 2005), and observations that affect the tropical mean state can be expected to have a memory of at least 10 days as it was seen for the impact of AMSU-A radiances on tropical wind forecast skill (Bormann et al., 2019).

Figure 4, in comparison with Figure 3, shows that differences between KWs in the two experiments occur at the locations of significant zonal wind shear. For example, the assimilation of Aeolus winds on May 13 enhanced easterlies near 100 hPa over Indian ocean. The vertical shape of analysis differences in Figure 4 exceeding 3 m/s at several locations suggests significant changes in the vertically propagating waves in UTLS. The vertical wave structure at two locations, 66°E and 90°E, and three consecutive days is presented in Figure 5. It shows the downward propagation of the KW phase from the lower stratosphere across the TTL. The vertical phase speed at 66°E earlier in the period has a greater amplitude than at 90°E. The most important feature is the modification of the KW zonal wind shear between 100 and 50 hPa where the amplitudes and the vertical propagation are the largest.

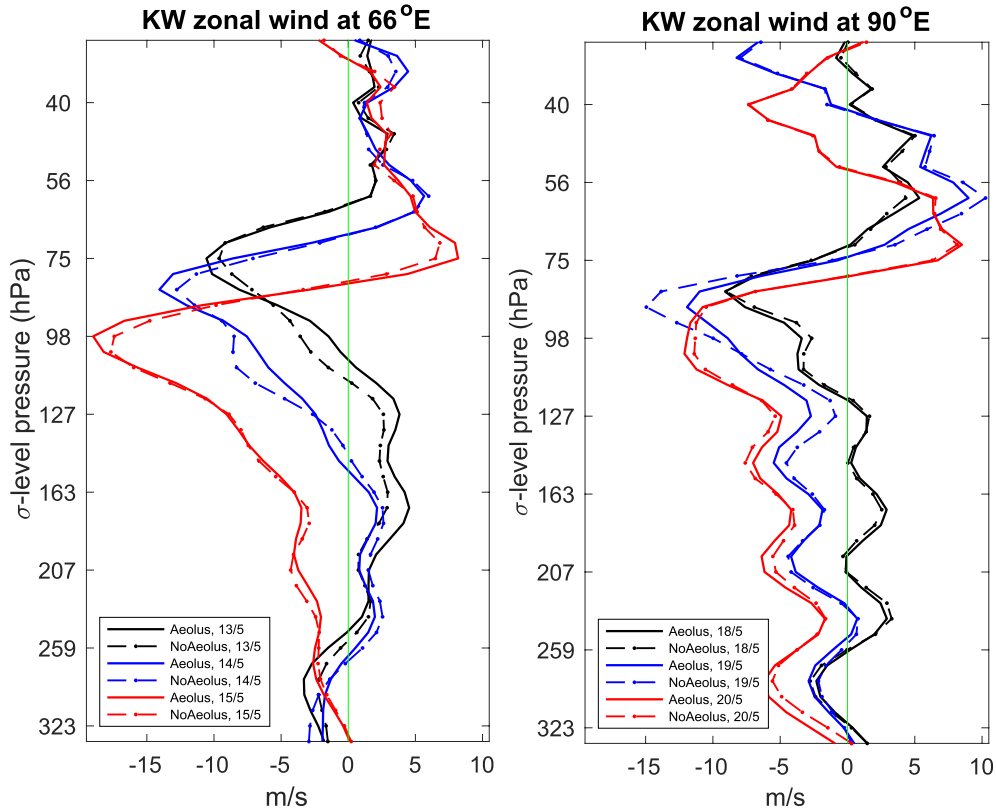

Figure 5. Kelvin wave zonal wind in 12 UTC analyses at three subsequent days in May 2020 in Aeolus (full lines) and NoAeolus (dashed lines) observing system experiments (OSEs). The locations are indicated above the panels.

The portion of the total zonal circulation associated with KWs exceeds the balanced zonal winds in the region of upper troposphere easterlies, but it is significantly smaller in the upper troposphere westerlies (Figure 3). This raises the question of the amplitudes of KW analysis increments with respect to analysis increments in balanced winds. If KW analysis increments are small, this may suggest that KWs are well represented in the short-range forecasts (background fields) in both experiments. However, evaluation of tropical analysis and forecast uncertainties do not support such an argument (Podglajen et al., 2014; Žagar, 2017). Current background errors estimated from the ensembles are not much lower than the ensemble estimates from 2015 discussed in Žagar (2017) and previously discussed growth of forecast errors associated with KWs is thus likely unchanged. Differences between the zonal wind in NoAeolus and Aeolus analyses on May 19, 2020 partitioned between balanced and unbalanced parts show that the two parts have similar amplitudes in regions and layers of strong shear, where westerlies shift to easterlies or vice versa. In other regions such as the upper troposphere westerlies over the Pacific with a weaker KW signal, differences between Aeolus and NoAeolus are almost entirely in balanced modes (Figure in Supporting Information S1).

Similar analysis as in Figure 5 for later dates in July and August shows that differences between Aeolus and NoAeolus are largest in the upper troposphere and TTL. Two examples in Supporting Information S1 show KWs profiles in mid-July and at the end of August, when the differences in Figure 1 are pronounced. In these cases, as well as in the other cases in August, the KW beneath the tropopause is propagating downward. This may partly explain a smaller effect of Aeolus winds on forecasts in August compared to May in Figure 2, which is seen also at 50 hPa level (not shown). Another possible reason is that KWs in the easterly balanced flow are better represented by the model in the NoAeolus experiment. There is scope for follow-on investigations using the sensitivity studies and looking at the analysis increments. A particularly interesting question is the extent to which the Aeolus winds are correcting model deficiencies in the TTL and higher up, that are discussed in Polichtchouk et al. (2021).

4. Discussion and Outlook

Aeolus HLOS winds in the tropics provide predominantly zonal wind information and their positive impact on tropical analyses has been foreseen (e.g., Tan & Andersson, 2004; Tan et al., 2007). However, during the two decades since the Aeolus project started, NWP experienced large advancements with improved data assimilation and more observations used, and the current global forecast models run at resolutions around 10 km, which is much better resolution than when Aeolus was first conceived. Yet, practical predictability in extratropics remains under 10 days (Haiden et al., 2018). Reduction of tropical analysis uncertainties and a more accurate representation of tropics-extratropics interactions are argued as one way to improve medium-range and extended-range forecasting (Žagar & Szunyogh, 2020).

Our evaluation of the tropical forecasts at 100 hPa as well as the background fit to other observations shows an overall positive impact of Aeolus winds in the tropics, in spite of large random errors in the Rayleigh-clear winds. In particular, we show that the impact on forecast quality lasted longer in May than later in summer, when the easterly QBO shear lines were weak and the easterly balanced winds were present in the whole tropical belt. The coupling between the phase of QBO and the assimilated Aeolus winds is likely through the KWs that were shown to explain a significantly larger forecast-error variance in the easterly QBO phase compared to the westerly phase (Žagar et al., 2007). While the QBO phase and KWs are not explicitly accounted for in the background-error term for data assimilation in the ECMWF system, the background-error variances are derived using the 4D-Var ensemble of data assimilations thereby accounting for the flow-dependent amplitudes of short-range forecast errors in temperature and winds. It remains to investigate how Aeolus winds affect analysis increments in the upper troposphere and TTL and the dispersiveness of the ensemble prediction system. Results presented here suggest that at least a part of reported forecast improvements in the tropical tropopause layer and the lower stratosphere is likely due to corrections to the large-scale, vertically propagating Kelvin waves in layers with a strong zonal wind shear.

Data Availability Statement

The source code of the ECMWF IFS model is not available for public use as it is intellectual property of the ECMWF and its member states. Global files with outputs of the modal decomposition of ECMWF OSEs discussed in the paper are available at https://zenodo.org/record/5207392#.YRvjby2w1Bw (doi:10.5281/zenodo.5207392).

Acknowledgments
We are indebted to the many experts who over years worked on the Aeolus mission until its launch on August 22, 2018, and to many who have been operating the satellite and contributing to the validation and processing of Aeolus measurements at ESA and within the Aeolus Data, Innovation, and Science Cluster (DISC) team. We thank Frank Sielmann and Wenlin Xiao of UHH for their help with processing outputs from MODES, and to three anonymous reviewers for their constructive comments. The MODES software can be requested through the MODES webpage http://modes.cen.uni-hamburg.de. Open access funding enabled and organized by Projekt DEAL.

References

Alexander, M. J., & Ortland, D. A. (2010). Equatorial waves in High Resolution Dynamics Limb Sounder (HIRDLS) data. *Journal of Geophysical Research*, *115*, D24111. https://doi.org/10.1029/2010JD014782

Andrews, D. G., Holton, J. R., & Leovy, C. B. (1987). *Middle atmosphere dynamics*. Academic Press, Inc.

Baars, H., Radenz, M., Floutsi, A. A., Engelmann, R., Althausen, D., Heese, B., et al. (2021). Californian wildfire smoke over Europe: A first example of the aerosol observing capabilities of Aeolus compared to ground-based lidar. *Geophysical Research Letters*, *48*, e2020GL092194. https://doi.org/10.1029/2020GL092194

Baker, W. E., Atlas, R., Cardinali, C., Clement, A., Emmitt, G. D., Gentry, B. M., et al. (2014). Lidar-measured wind profiles—The missing link in the global observing system. *Bulletin of the American Meteorological Society*, *95*, 543–564. https://doi.org/10.1175/bams-d-12-00164.1

Baldwin, M. P., & Gray, L. J. (2005). Tropical stratospheric zonal winds in ERA-40 reanalysis, rocketsonde data, and rawinsonde data. *Geophysical Research Letters*, *32*, L09806. https://doi.org/10.1029/2004GL022328

Baldwin, M. P., Gray, L. J., Dunkerton, T. J., Hamilton, K., Haynes, P. H., Randel, W. J., et al. (2001). The quasi-biennial oscillation. *Reviews of Geophysics*, *39*, 179–229. https://doi.org/10.1029/1999RG000073

Banyard, T. P., Wright, C. J., Hindley, N. P., Halloran, G., Krisch, I., Kaifler, B., & Hoffmann, L. (2021). Atmospheric gravity waves in Aeolus Wind Lidar observations. *Geophysical Research Letters*, *48*, e2021GL092756. https://doi.org/10.1029/2021GL092756

Bauer, P., Thorpe, A., & Brunet, G. (2015). The quiet revolution of numerical weather prediction. *Nature*, *525*(47), 47–55. https://doi.org/10.1038/nature14956

Blaauw, M., & Žagar, N. (2018). Multivariate analysis of Kelvin wave seasonal variability in ECMWF L91 analyses. *Atmospheric Chemistry and Physics*, *18*, 8313–8330. https://doi.org/10.5194/acp-18-8313-2018

Bormann, N., Lawrence, H., & Farnan, J. (2019). *Global observing system experiments in the ECMWF assimilation system* (ECMWF Research Department Technical Memorandum 839). Retrieved from https://www.ecmwf.int/node/18859

ESA. (1999). *Atmospheric dynamics mission, reports for mission selections* (ESA SP-1233, Vol. *4*, p. 155).

ESA. (2008). *ADM-Aeolus science report* (ESA SP-1311, p. 121).

Fisher, M., Leutbecher, M., & Kelly, G. (2005). On the equivalence between Kalman smoothing and weak-constraint four-dimensional variational data assimilation. *Quarterly Journal of the Royal Meteorological Society*, *131*, 3235–3246. https://doi.org/10.1256/qj.04.142

Flannaghan, T. J., & Fueglistaler, S. (2012). Tracking Kelvin waves from the equatorial troposphere into the stratosphere. *Journal of Geophysical Research*, *117*, D21108. https://doi.org/10.1029/2012JD017448

Flannaghan, T. J., & Fueglistaler, S. (2013). The importance of the tropical tropopause layer for equatorial Kelvin wave propagation. *Journal of Geophysical Research: Atmospheres*, *118*, 5160–5175. https://doi.org/10.1002/jgrd.50418

Fujiwara, M., Suzuki, J., Gettelman, A., Hegglin, M., Akiyoshi, H., & Shibata, K. (2012). Wave activity in the tropical tropopause layer in seven reanalysis and four chemistry climate model data sets. *Journal of Geophysical Research*, *117*, D12105. https://doi.org/10.1029/2011JD016808

Haiden, T., Janousek, M., Bidlot, J., Buizza, R., Ferranti, L., Prates, F., & Vitart, F. (2018). *Evaluation of ECMWF forecasts, including the 2018 upgrade* (ECMWF technical memo 831). Retrieved from http://www.ecmwf.int

Kasahara, A. (2020). 3D Normal Mode Functions (NMFs) of a global baroclinic atmospheric model. In N. Žagar, & J. Tribbia (Eds.), *Modal view of atmospheric variability: Applications of normal-mode function decomposition in weather and climate research* (Mathematics of Planet Earth Series, Vol. *8*). Springer. https://doi.org/10.1007/978-3-030-60963-4_1

Kasahara, A., & Puri, K. (1981). Spectral representation of three-dimensional global data by expansion in normal mode functions. *Monthly Weather Review*, *109*, 37–51. https://doi.org/10.1175/1520-0493(1981)109<0037:srotdg>2.0.co;2

Kim, H., Caron, J. M., Richter, J. H., & Simpson, I. R. (2020). The lack of QBO-MJO connection in CMIP6 models. *Geophysical Research Letters*, *47*, e2020GL087295. https://doi.org/10.1029/2020GL087295

Kim, J. E., & Alexander, M. J. (2013). Tropical precipitation variability and convectively coupled equatorial waves on submonthly timescales in reanalyses and TRMM. *Journal of Climate*, *26*, 3013–3030. https://doi.org/10.1175/jcli-d-12-00353.1

Lean, P., Holm, E. V., Bonavita, M., Bormann, N., McNally, A. P., & Järvinen, H. (2021). Continuous data assimilation for global numerical weather prediction. *Quarterly Journal of the Royal Meteorological Society*, *147*, 273–288. https://doi.org/10.1002/qj.3917

Park, Y.-Y., Buizza, R., & Leutbecher, M. (2004). TIGGE: Preliminary results on comparing and combining ensembles. *Quarterly Journal of the Royal Meteorological Society*, *134*, 2029–2050.

Podglajen, A., Hertzog, A., Plougonven, R., & Žagar, N. (2014). Assessment of the accuracy of (re)analyses in the equatorial lower stratosphere. *Journal of Geophysical Research: Atmospheres*, *119*, 11166–11188. https://doi.org/10.1002/2014JD021849

Polichtchouk, I., Bechtold, P., Bonavita, M., Forbes, R., Healy, S., Hogan, R., et al. (2021). *Stratospheric modelling and assimilation* (ECMWF TM 877). Retrieved from https://www.ecmwf.int/node/19875

Reitebuch, O. (2012). The spaceborne Wind Lidar mission ADM-Aeolus. In U. Schumann (Ed.), *Atmospheric physics: Research topics in aerospace* (pp. 815–827). Springer. https://doi.org/10.1007/978-3-642-30183-4_49

Rennie, M., & Isaksen, L. (2020). *The NWP impact of Aeolus level-2B winds at ECMWF* (ECMWF Research Department Technical Memorandum 864). https://doi.org/10.21957/alift7mhr

Rennie, M., Isaksen, L., Weiler, F., de Kloe, J., Kanitz, T., & Reitebuch, O. (2021). The impact of Aeolus wind retrievals in ECMWF global weather forecasts. *Quarterly Journal of the Royal Meteorological Society*, *147*, 3555–3586. https://doi.org/10.1002/qj.4142

Salby, M. L., & Garcia, R. R. (1987). Transient response to localized episodic heating in the tropics. Part I: Excitation and short-time near-field behavior. *Journal of the Atmospheric Sciences*, *44*, 458–498. https://doi.org/10.1175/1520-0469(1987)044<0458:trtleh>2.0.co;2

Šavli, M., Žagar, N., & Anderson, J. (2018). Assimilation of the horizontal line-of-sight winds with a mesoscale EnKF data assimilation system. *Quarterly Journal of the Royal Meteorological Society*, *144*, 2133–2155. https://doi.org/10.1002/qj.3323

Sobel, A., Polvani, N., & Nilsson, J. (2001). The weak temperature gradient approximation. *Journal of the Atmospheric Sciences*, *58*, 1473–1489. https://doi.org/10.1175/1520-0469(2001)058<3650:twtgaa>2.0.co;2

Stoffelen, A., Pailleux, J., Källén, E., Vaughan, J. M., Isaksen, L., Flamant, P., et al. (2005). The atmospheric dynamic mission for global wind measurements. *Bulletin of the American Meteorological Society*, *86*, 73–88. https://doi.org/10.1175/bams-86-1-73

Suzuki, J., & Shiotani, M. (2008). Space-time variability of equatorial Kelvin waves and intraseasonal oscillations around the tropical tropopause. *Journal of Geophysical Research*, *113*, D16110. https://doi.org/10.1029/2007JD009456

Suzuki, J., Shiotani, M., & Nishi, N. (2010). Lifetime and longitudinal variability of equatorial Kelvin waves around the tropical tropopause region. *Journal of Geophysical Research*, *115*, D03103. https://doi.org/10.1029/2009JD012261

Tan, D., & Andersson, E. (2004). *Expected benefit of wind profiles from the ADM-Aeolus in a data assimilation system* (Final report for ESA contract No. 15342/01//NL/MM).

Tan, D., Andersson, E., De Kloe, J., Marseille, G.-J., Stoffelen, A., Denneulin, P. P. M., et al. (2008). The ADM-Aeolus wind retrieval algorithms. *Tellus A*, *60*, 191–205. https://doi.org/10.1111/j.1600-0870.2007.00285.x

Tan, D., Andersson, E., Fisher, M., & Isaksen, L. (2007). Observing-system impact assessment using a data assimilation ensemble technique: Application to the ADM-Aeolus wind profiling mission. *Quarterly Journal of the Royal Meteorological Society*, *133*, 381–390. https://doi.org/10.1002/qj.43

Vitart, F., Balsamo, G., Buizza, R., Ferranti, L., Keeley, S., Magnusson, L., & Weisheimer, A. (2014). *Sub-seasonal predictions* (Vol. *734*, p. 47). ECMWF Research Department Technical Memorandum.

Wallace, J. M., & Kousky, V. E. (1968). Observational evidence of Kelvin waves in the tropical stratosphere. *Journal of the Atmospheric Sciences*, *25*, 900–907. https://doi.org/10.1175/1520-0469(1968)025<0900:oeokwi>2.0.co;2

Wheeler, M., & Kiladis, G. N. (1999). Convectively coupled equatorial waves: Analysis of clouds and temperature in the wavenumber-frequency domain. *Journal of the Atmospheric Sciences*, *56*, 374–399. https://doi.org/10.1175/1520-0469(1999)056<0374:ccewao>2.0.co;2

Wheeler, M., Kiladis, G. N., & Webster, P. J. (2000). Large-scale dynamical fields associated with convectively coupled equatorial waves. *Journal of the Atmospheric Sciences*, *57*, 613–640. https://doi.org/10.1175/1520-0469(2000)057<0613:lsdfaw>2.0.co;2

Žagar, N. (2017). A global perspective of the limits of prediction skill of NWP models. *Tellus A*, *69*, 1317573.

Žagar, N., Andersson, E., Fisher, M., & Untch, A. (2007). Influence of the quasi-biennial oscillation on the ECMWF model short-range forecast errors in the tropical stratosphere. *Quarterly Journal of the Royal Meteorological Society*, *133*, 1843–1853.

Žagar, N., Blaauw, M., Jesenko, B., & Magnusson, L. (2016). *Diagnosing model performance in the tropics* (Vol. *147*). ECMWF Newsletter. Retrieved from http://www.ecmwf.int/publications/newsletters

Žagar, N., Buizza, R., & Tribbia, J. (2015). A three-dimensional multivariate modal analysis of atmospheric predictability with application to the ECMWF ensemble. *Journal of the Atmospheric Sciences*, *72*, 4423–4444.

Žagar, N., Isaksen, L., Tan, D., & Tribbia, J. (2013). Balance properties of the short-range forecast errors in the ECMWF 4D-Var ensemble. *Quarterly Journal of the Royal Meteorological Society*, *139*, 1229–1238.

Žagar, N., Kasahara, A., Terasaki, K., Tribbia, J., & Tanaka, H. L. H. (2015). Normal-mode function representation of global 3D datasets: Open-access software for the atmospheric research community. *Geoscientific Model Development*, *8*, 1169–1195.

Žagar, N., Stoffelen, A., Marseille, G.-J., Accadia, C., & Schlüssel, P. (2008). Impact assessment of simulated Doppler Wind Lidars with a multivariate variational assimilation in the tropics. *Monthly Weather Review*, *136*, 2443–2460.

Žagar, N., & Szunyogh, I. (2020). Comments on "What is the predictability limit of midlatitude weather?" *Journal of the Atmospheric Sciences*, *72*(2), 781–785. https://doi.org/10.1175/JAS-D-19-0166.1

Zhang, C. (2005). Madden-Julian oscillation. *Reviews of Geophysics*, *43*, RG2003. https://doi.org/10.1029/2004RG000158